In this sequence, the log of $(S_\infty - S_t)$ is plotted against t where S_∞ and S_t are the transformed signals from the $90°_\infty$ and $90°_t$ pulses, thus yielding only positive peaks in the spectral display. T_1 is the time, t, at which the linear trace of $(S_\infty - S_t)$ reaches 0.368 ($\equiv 1/e$) of $(S_\infty - S_t)$ for $t = 0$ ($\equiv 2S_\infty$). For each determination 6–10 sets of measurements were taken. Some determinations were repeated on different samples of the same compound. Reproducibility of T_1 values was considerably better than $\pm 15\%$ in most cases. Accuracy limitations depend in each instance on solute concentration and the length of data acquisition. In the higher accuracy studies (stated probable error limits $<10\%$) very high signal-to-noise ratios were achieved. Repetitive experiments on separate, equivalent samples yielded T_1 values within one-third to one-half the stated maximum probable error limits.

NOE Measurements. Direct $^{29}Si-^{1}H$ NOE determinations were obtained from continuous wide-band and pulse-modulated[2a,37] wide-band proton decoupled ^{29}Si spectra. Using the technique of decoupling just before the short ^{29}Si pulses and during short (<2 sec) acquisitions of the free-induction decays while leaving the decoupler off for the long ($\gtrsim 4T_1$) pulse intervals allowed direct measurements of the NOE's from all of the ^{1}H decoupled spectra (where ^{29}Si T_1's > 20 sec). A few of the early NOE determinations were obtained from decoupled and coupled spectra.[2a] Most NOE's are reported to an accuracy of $\pm 0.1\eta$.

Acknowledgments. We thank Charles S. Peters for writing supplementary computer software and Craig D. Robertson for experimental assistance. We also thank Professor F. A. L. Anet for several helpful discussions.

(37) R. Freeman, H. D. W. Hill, and R. Kaptein, *J. Magn. Resonance*, 7, 327 (1972).

Decomposition Kinetics of Chemically Activated Dimethylsilane and Ethylsilane[1]

W. L. Hase, C. J. Mazac, and J. W. Simons*

Contribution from the Chemistry Department, New Mexico State University, Las Cruces, New Mexico 88003. *Received October 26, 1972*

Abstract: An experimental study of the decomposition kinetics of chemically activated dimethylsilane and ethylsilane produced by reaction of singlet methylene with methylsilane is reported. Rate constants for various possible decomposition paths are deduced and a RRKM theoretical treatment of CH_3–Si bond rupture is given. Revised theoretical calculations for previous studies of CH_3–Si bond rupture are presented.

The relative importance of possible primary decomposition paths of ground electronic state silanes and alkylsilanes is an important question toward which a few recent pyrolysis[2] and chemical activation[3] studies have been directed. Some possible indications of criteria for decisions on the relative contributions of radical production (bond rupture) and molecular elimination have resulted.[4] In view of the major difficulties which have plagued thermal decomposition studies in the past, namely heterogeneous effects and complicating secondary reactions, chemical activation studies of these decomposition processes are of value. The relatively low temperature, at which chemical activation studies can be carried out, tends to minimize many heterogeneous complications and homogeneous secondary reactions.

The production of chemically activated dimethylsilane and ethylsilane by Si–H and C–H insertion respectively of singlet methylene with methylsilane has been reported.[5] That work is extended here, with more complete product analyses, to lower pressures.

Experimental Section

Materials. The acquisition and handling procedures for diazomethane (DM), methylsilane (MS), *n*-butane (nB), 1,3-butadiene (Bd), and oxygen have been described in earlier work.[3,5]

Apparatus. The gas handling vacuum system, photolysis radiation source, and Pyrex reactors have been described.[3]

Procedure. The following mixtures were photolyzed at 3660 Å and 25° for various times depending on the total pressure: $CH_2N_2/CH_3SiH_3/O_2$, 1/10/1; $CH_2N_2/CH_3SiH_3/n\text{-}C_4H_{10}/O_2$, 1/7.5/2.5/1; $CH_2N_2/CH_3SiH_3/n\text{-}C_4H_{10}/1,3\text{-}C_4H_6$, 1/2/2/4; and $CH_2N_2/CH_3SiH_3/1,3\text{-}C_4H_6$, 1/3/6. Total pressures ranged from 1 to 200 cm. After photolysis the reaction mixtures were fractionated by vacuum distillation at −196°. The noncondensibles were collected with a Toepler pump and analyzed by glpc or mass spectrometry. The condensibles were analyzed by glpc.

Analytical. In the early experiments the noncondensibles were analyzed by glpc on a 10-ft molecular sieve (5 A) column. This proved unsatisfactory since quantitative transfer of the noncondensibles to and from sample tubes and to the glpc was difficult. Consequently a mass spectrometric analysis was devised which did not require quantitative transfer in order to get complete product ratios. A sample of a known mixture of argon and *n*-butane was added to each product plus reaction mixture just prior to removal of the noncondensibles. This procedure was used only for those reactions in which *n*-butane was not initially added as an internal monitor of total $^{1}CH_2$ insertion. The noncondensibles at −196° (H_2, CH_4, N_2, Ar, O_2) were quantitatively collected with a Toepler pump and analyzed mass spectrometrically which quantitatively gave H_2 and CH_4 relative to argon. The

(1) The National Science Foundation is gratefully acknowledged for financial support.

(2) (a) E. M. Tebben and M. A. Ring, *Inorg. Chem.*, **8**, 1787 (1969); J. J. Kohanek, P. Estacio, and M. A. Ring, *ibid.*, **8**, 2516 (1969); M. A. Ring, M. I. Puentes, and H. E. O'Neal, *J. Amer. Chem. Soc.*, **92**, 4845 (1970); M. A. Ring, R. B. Baird, and P. Estacio, *Inorg. Chem.*, **9**, 1004 (1970); P. Estacio, M. D. Sefcik, E. K. Chan, and M. A. Ring, *ibid.*, **9**, 1068 (1970); R. B. Baird, M. D. Sefcik, and M. A. Ring, *ibid.*, **10**, 883 (1971); (b) J. H. Purnell and R. Walsh, *Proc. Roy. Soc., Ser. A*, **293**, 543 (1966); M. Bowery and J. H. Purnell, *J. Amer. Chem. Soc.*, **92**, 2594 (1970); (c) H. Sakurai, A. Hosemi, and M. Kumada, *Chem. Commun.*, 4, (1969); (d) W. H. Atwell and D. R. Weyenberg, *J. Amer. Chem. Soc.*, **90**, 3438 (1968); W. H. Atwell, L. G. Mahone, S. F. Hayes, and J. G. Uhlmann, *J. Organometal. Chem.*, **18**, 69 (1969); (e) I. M. T. Davidson and C. A. Lambert, *Chem. Commun.*, 1276 (1969); I. M. T. Davidson and C. A. Lambert, *J. Chem. Soc. A*, 882 (1971).

(3) (a) W. L. Hase and J. W. Simons, *J. Chem. Phys.*, **52**, 4004 (1970); (b) W. L. Hase and J. W. Simons, *J. Organometal. Chem.*, **32**, 47 (1971); (c) W. L. Hase, W. G. Brieland, P. W. McGrath, and J. W. Simons, *J. Phys. Chem.*, **76**, 459 (1972).

(4) (a) R. A. Jackson, *Advan. Free-Radical Chem.*, **3**, 231 (1969); (b) I. M. T. Davidson, *J. Organometal. Chem.*, **24**, 97 (1970).

(5) C. J. Mazac and J. W. Simons, *J. Amer. Chem. Soc.*, **90**, 2484 (1968).

glpc analyses of the condensibles gave the condensible products relative to the added *n*-butane. All product ratios were then easily determined from the known argon/*n*-butane ratio.

A Hitachi RMU-6E mass spectrometer was calibrated with a known mixture immediately before and after a series of unknown noncondensible analyses. The condensibles were initially analyzed by glpc at 25° on a 10-ft column of 30% dibutyl phthalate on Chromosorb. This column provided analyses for the higher boiling components. The effluent from this column was trapped at −196° and further analyzed at 25° on a glpc column consisting of 25 ft of 30% dibutyl phthalate on Chromosorb with a 4-ft extension of 30% dibutyl phthalate on Chromosorb with a 4-ft extension of 30% didecyl phthalate on Chromosorb. This column provided analyses for the lower boiling components. Ethane and ethylene were unresolved by the above column so their combined peak was trapped at −196° along with the *n*-butane (added with argon prior to analysis) peak. This sample was analyzed at 25° on a column consisting of 25 ft of 30% dinonyl phthalate and 30 ft of 30% $AgNO_3$/butanediol on Chromosorb. All columns were calibrated with known mixtures similar in composition to reactant plus product mixtures.

Dark reactions were submitted to the analytical scheme periodically. For reactions in which O_2 was added some H_2 was formed by dark reaction. No dark reaction products of interest were observed in the other systems.

All product identifications were by comparison of glpc retention times and mass spectra with those of authentic samples. The higher molecular weight organosilanes identified in this work were also produced by mercury photosensitization of the appropriate mixtures. In this way methyldisilane was produced from methylsilane and silane (1:1), methylethylsilane from methylsilane and ethane (1:15), *sec*-butylsilane and *n*-butylsilane simultaneously from silane and *n*-butane (1:5), 1,2-dimethyldisilane from pure methylsilane, 1,1,2-trimethyldisilane from dimethylsilane and methylsilane (1:1), and methylethyldisilane from methylsilane and ethylsilane (1:1).

Results

Products. The products observed from photolysis of DM/MS mixtures at low pressures (1–10 cm) were hydrogen, methane, ethane, dimethylsilane (DMS), ethylsilane (ES), methyldisilane (MDS), methylethylsilane (MES), 1,2-dimethyldisilane (DMDS), 1,3-dimethyltrisilane (DMTS), 1,1,2-trimethyldisilane (TMDS), 1-methyl-2-ethyldisilane (MEDS), and 1,1,3-trimethyltrisilane (TMTS). Upon addition of *n*-butane to the reactant mixtures, as a monitor of total $^1CH_2$ reaction, the expected C–H insertion products, isopentane and *n*-pentane, were observed as well as a trace of *sec*-butylsilane. Addition of oxygen to the reaction mixtures eliminated MES and the amounts of ES, DMS, TMDS, MEDS, TMTS, C_2H_6, and CH_4 were reduced relative to the pentanes. This latter result suggests that these products are formed in part by reactions of triplet and/or doublet radicals and in part by molecular reactions. The amount of ES was unaffected relative to the pentanes at high pressures (>10 cm). As mentioned earlier, O_2 addition produces H_2 in a slow dark reaction with methylsilane so the effect of O_2 on the photochemical production of H_2 was ambiguous. Addition of 1,3-butadiene (Bd) as a radical scavenger decreased the amounts of H_2, CH_4, C_2H_6, ES, and DMS relative to the pentanes. High molecular weight products were not determined in the Bd experiments. It was found that ~15% O_2 or a ratio of Bd/MS = 2 was sufficient for complete scavenging; *i.e.*, addition of larger amounts led to no further changes in observed product proportions.

Qualitatively, the products that were observed to decrease with increasing pressure (in the presence of a scavenger) were H_2, CH_4, C_2H_6, MDS, DMDS, DMTS, TMDS, MEDS, and TMTS. The products observed to increase with increasing pressure were DMS and ES. The quantitative behavior of H_2, CH_4, C_2H_6, DMS, and ES is discussed in the next section. Quantitative information on the higher molecular weight products was not obtained since their amounts were small and the analyses for them were rather insensitive.

Discussion

Experimental Results. The following proposed mechanism satisfactorily explains the observed products and their variations.

$$CH_2N_2 + h\nu \longrightarrow CH_2 + N_2 \quad (1)$$

$$CH_2 + CH_3SiH_3 \longrightarrow (CH_3)_2SiH_2^* \quad (2)$$

$$\longrightarrow CH_3CH_2SiH_3^* \quad (3)$$

$$\longrightarrow CH_3 + CH_3SiH_2 \quad (4)$$

$$(CH_3)_2SiH_2^* \longrightarrow CH_3 + CH_3SiH_2 \quad (5)$$

$$\longrightarrow CH_4 + CH_3SiH \quad (6)$$

$$\longrightarrow (CH_3)_2Si + H_2 \quad (7)$$

$$\longrightarrow (CH_3)_2SiH + H \quad (8)$$

$$\xrightarrow{W} (CH_3)_2SiH_2 \quad (9)$$

$$CH_3CH_2SiH_3^* \longrightarrow CH_3CH_2 + SiH_3 \quad (10)$$

$$\longrightarrow CH_3CH_2SiH + H_2 \quad (11)$$

$$\longrightarrow CH_3CH_2SiH_2 + H \quad (12)$$

$$\longrightarrow C_2H_6 + SiH_2 \quad (13)$$

$$\xrightarrow{W} CH_3CH_2SiH_3 \quad (14)$$

An asterisk represents excess vibrational–internal rotational energy above that required for decomposition and W represents the collision frequency. The relevant collision frequency calculations are presented in Appendix I. There are, of course, many possible secondary reactions of the various radicals produced in the mechanism, and these no doubt contribute to the products in the absence of a radical scavenger. The symbol CH_2 is used here to represent either singlet or triplet methylene or a mixture of both. Reaction 1 produces a mixture, reactions 2 and 3 probably involve only singlet CH_2, and reaction 4 probably involves both singlet and triplet. The singlet–triplet methylene reactivity question in alkylsilane systems is discussed and referenced in ref 3. There is evidence that silicon diradicals, such as SiH_2, CH_3SiH, $(CH_3)_2Si$, and CH_3CH_2SiH, are singlets[6] which insert readily into Si–H bonds.[2,7] These singlets presumably are not efficiently scavenged by radical scavengers. The products MDS, MDS, TMDS, and MEDS in the presence of O_2 as a scavenger can be explained by the insertion into a Si–H bond of CH_3SiH_3 by SiH_2, CH_3SiH, $(CH_3)_2Si$, and CH_3CH_2SiH, respectively.

It is quite likely that considerably more H_2 results from reaction 7 than from reaction 11 in the scavenged systems. This is consistent with $k_2/k_3 \sim 8$[5] and the reasonable assumption that at the same energy ($E^*_{DMS} = E^*_{ES}$) $k_{11} \sim 3k_7$, where the 3 accounts for reaction

(6) I. Dubois, G. Herzberg, and R. D. Varma, *J. Chem. Phys.*, **47**, 4262 (1967).

(7) K. Obi, A. Clement, H. E. Gunning, and O. P. Strausz, *J. Amer. Chem. Soc.*, **91**, 1622 (1969); M. A. Ring, G. D. Beverly, F. H. Koester, and R. P. Hollandsworth, *Inorg. Chem.*, **8**, 2033 (1969).

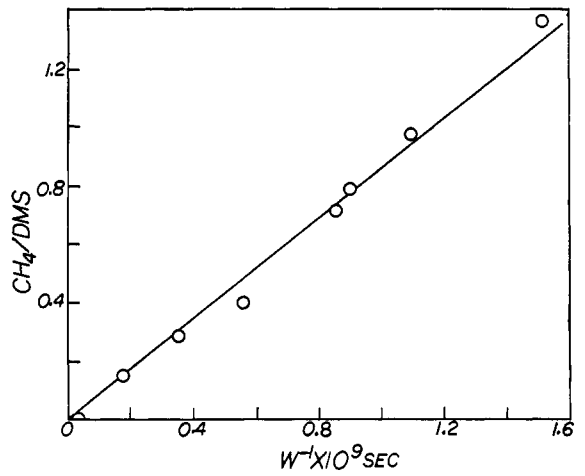

Figure 1. A plot of CH_4/DMS *vs.* W^{-1} for CH_2N_2/MS/Bd photolyses at 3660 Å.

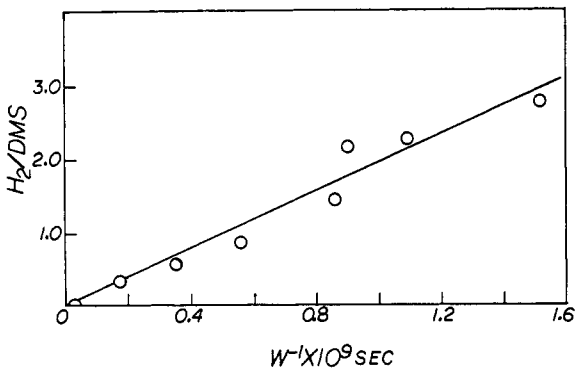

Figure 2. A plot of H_2/DMS *vs.* W^{-1} for CH_2N_2/MS/Bd photolyses at 3660 Å.

path degeneracy. An argument analogous to that presented previously[3c] indicates that $E^*_{DMS} \sim E^*_{ES} + 7$ kcal/mol; thus $k_{11} \sim k_7$ and the H_2 from reaction 11 would be only about one-eighth the H_2 from reaction 7. Our measured value of TMDS/MEDS $\sim$ 10 in scavenged systems supports this interpretation.

Reactions 6, 7, and 13 explain the formation in the scavenged experiments of CH_4, H_2, and C_2H_6, respectively, at low pressures and their decrease with increasing pressure. The collisional stabilization reactions 9 and 14 increase proportionally in relative importance with increasing pressure. A steady-state treatment of DMS* and ES* results in eq I–III for the

$$\frac{CH_4}{DMS} = \frac{k_6}{W} \quad \text{(I)}$$

$$\frac{H_2}{DMS} = \frac{k_7}{W} \quad \text{(II)}$$

$$\frac{C_2H_6}{ES} = \frac{k_{13}}{W} \quad \text{(III)}$$

quantitative behavior of CH_4, H_2, and C_2H_6, respectively, from reactions with added scavengers. The data plotted according to these equations are presented in Figures 1–3, respectively. The linearity of the data in Figures 1–3 along with the near-zero intercepts indicate that H_2, CH_4, and C_2H_6 are formed, in the presence of a scavenger, by molecular elimination

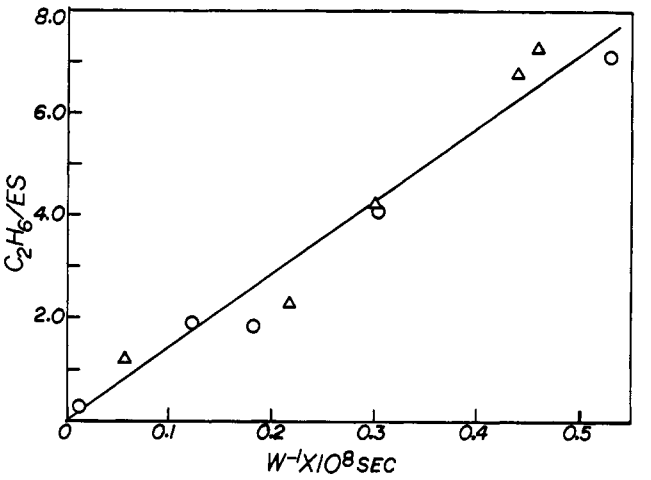

Figure 3. A plot of C_2H_6/ES *vs.* W^{-1} for (△) CH_2N_2/MS/Bd and (○) CH_2N_2/MS/O_2 photolyses at 3660 Å.

from DMS* and ES*. The derived values of k_6, k_7, and k_{13} are presented in Table I. Some comment

Table I. Decomposition Paths and Rate Constants for DMS* and ES*

Reaction		Rate, sec^{-1}	Eq no.
DMS*	→ products	$k_{DMS} = 4.0 \times 10^9$	
	→ $CH_3 + CH_3SiH_2$	$k_5 = [0.90 \times 10^9]^a$	5
	→ $CH_4 + CH_3SiH$	$k_6 = 0.85 \times 10^9$	6
	→ $(CH_3)_2Si + H_2$	$k_7 = 1.90 \times 10^9$	7
	→ $(CH_3)_2SiH + H$	$k_8 = [0.30 \times 10^9]^a$	8
ES*	→ products	$k_{ES} = 8.5 \times 10^9$	
	→ $CH_3CH_2 + SiH_3$	$k_{10} = [0.78 \times 10^9]^d$	10
	→ $CH_3CH_2SiH + H_2$	$k_{11} = [1.9 \times 10^9]^b$	11
	→ $CH_3CH_2SiH_2 + H$	$k_{12} = [0.14 \times 10^9]^c$	12
	→ $C_2H_6 + SiH_2$	$k_{13} = 1.4 \times 10^9$	13
	→ $C_2H_4 + SiH_4$	$k_{17} = [4.3 \times 10^9]^e$	17

[a] These rates were derived from previous theoretical results[3c] for $(CH_3)_3SiH^*$ (TMS*) decomposition by assuming $k_5/k_8 = 1/3$ times the ratio of k(methyl rupture) to k(H-atom rupture) for TMS*, and $k_{DMS} = k_5 + k_6 + k_7 + k_8$. The ratio, 1/3, accounts for the reaction path degeneracy ratio. [b] This rate was deduced by assuming $k_7/k_{11} = 1/3$ times the ratio of k(DMS*) to (ES*) per path for identical DMS* and ES* decomposition paths. The ratio k(DMS*)/k(ES*), per path was assumed to be about the same as the theoretical k(TMS*)/k(MES*) 3 from previous work.[3c] [c] k_{12} was deduced by a procedure similar to b. Thus $k_{12} = (1/3)k_8(3/2)$, where 3/2 is the reaction degeneracy ratio for reaction 12 to reaction 8. [d] $k_{10} = 5(1/3)k_{12}(k_5/k_8)$, where 5 is the theoretical ratio of ethyl to methyl rupture rates per path found previously[3a,c] and 1/3 is the reaction path degeneracy ratio for reaction 10 to reaction 12. [e] $k_{17} = k_{ES} - k_{10} - k_{11} - k_{12} - k_{13}$.

on the effectiveness of butadiene as an H-atom scavenger in this system is worthwhile since our conclusions concerning molecular elimination of H_2, reactions 7 and 11, rest on the H atom producing reactions 8 and 12 not being followed, in the presence of excess butadiene, by H-atom abstraction from methylsilane by the formed H atoms. Experimentally we found that increasing porportions of butadiene reduced H_2 yields up to a Bd/Ms ratio of ~2 with no further reduction upon further addition of butadiene. Recently it has been found that D atoms add 1.72 times faster to C_2D_4 than they abstract from methylsilane.[8] This result combined with an earlier measure-

(8) K. Obi, H. S. Sandhu, H. E. Gunning, and O. P. Strausz, *J. Phys. Chem.*, 76, 3911 (1972).

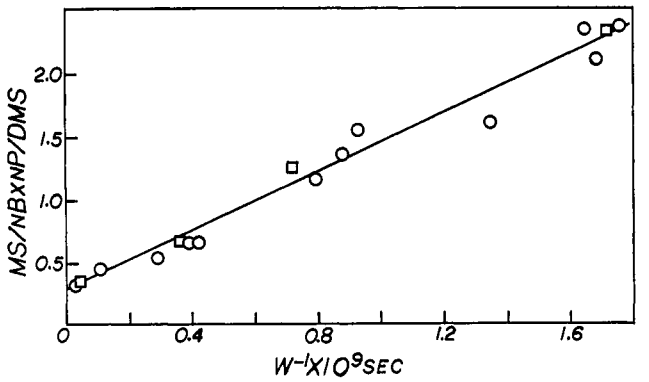

Figure 4. A plot of nP/DMS × MS/nB *vs.* W^{-1} for (□) CH_2N_2/MS/nB/Bd and (○) CH_2N_2/MS/nB/O_2 photolyses at 3660 Å. The intercept has been determined and discussed previously.[5]

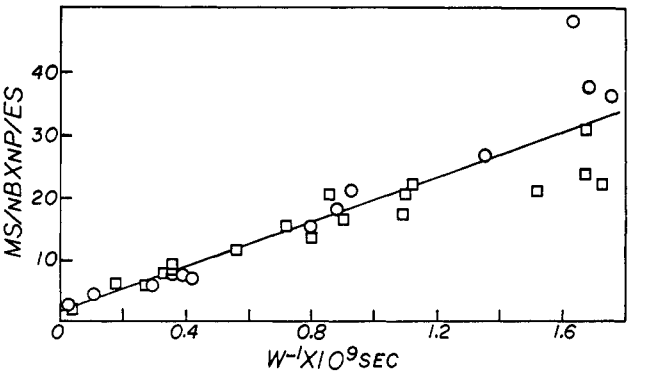

Figure 5. A plot of nP/ES × MS/nB *vs.* W^{-1} for (□), CH_2N_2/MS/nB/Bd and (○) CH_2N_2/MS/nB/O_2 photolyses at 3660 Å. The intercept has been determined and discussed previously.[5]

ment of 7.5 for the relative H-atom addition rate to butadiene and ethylene[9] yields 13 for the H-atom addition rate to butadiene relative to abstraction from methylsilane. Thus in our system <4% of the H atoms produced would abstract from methylsilane.

Addition of *n*-butane (nB) to the reaction mixtures in the presence of a scavenger leads to the formation of isopentane and *n*-pentane by reactions 15 and 16.

$$CH_2 + n\text{-}C_4H_{10} \longrightarrow (CH_3)_2CHCH_2CH_3 \text{ (IP)} \quad (15)$$

$$\longrightarrow CH_3(CH_2)_3CH_3 \text{ (nP)} \quad (16)$$

The pentanes are initially chemically activated but are completely stabilized at the lowest pressures of this study.[10] The IP/nP ratio from these experiments was in agreement with previous determinations. Equations 4 and 5 result from application of the steady-state approximation to DMS* and ES*, respectively, in the mechanism. The data plotted according to eq IV and V are given in Figures 4 and 5, respectively

$$\frac{nP}{DMS}\frac{MS}{nB} = \frac{k_{16}}{k_2} + \frac{k_{DMS}k_{16}}{W\,k_2} \quad (IV)$$

$$\frac{nP}{ES}\frac{MS}{nB} = \frac{k_{16}}{k_3} + \frac{k_{ES}k_{16}}{W\,k_3} \quad (V)$$

where $k_{DMS} = k_5 + k_6 + k_7 + k_8$ and $k_{ES} = k_{10} + k_{11} + k_{12} + k_{13}$. The correspondence in Figures 3–5 between the data for oxygen- and butadiene-scavenged reactions is gratifying and suggests no other effects of the scavengers are important. The value of k_{ES} derived from Figure 5 has a rather large uncertainty. This is due to the small amount of ES formed and the fact that its peak was not well resolved from the DMS peak tail in the glpc analysis.

Several other rate constants for proposed decomposition paths (k_5, k_8, k_{10}, k_{11}, k_{12}, k_{17}) are derived in Table I. These rates were deduced from the present results and previous experimental and theoretical results,[3c] as described in the footnotes to Table I. It is emphasized that these derived rates are quite tentative but should represent reasonable estimates.

Reaction 17 is proposed to account for the half of k_{ES} that is not accounted for by the other likely paths, k_{10} to k_{13}. An experimental test for reaction 17 would be difficult since reaction 3 is only one-eighth as fast as reaction 2 and thus the amounts of C_2H_4 and SiH_4 from reaction 17 would be quite small. Gas-phase diazomethane photolysis systems always produce some C_2H_4 in any case. Evidence for reactions similar to reaction 17 in the decomposition haloalkylsilanes[11] provides some indirect weak support for its occurrence here.

Theoretical Considerations. RRKM[12] theory has proven to be successful in quantitatively describing the specific decomposition rates, k_E, of chemically activated molecules. An RRKM theory calculation of k_E requires a knowledge of the decomposition path, the value of the critical energy, E_0, for decomposition, the value of the excitation energy, E^*, of the chemically activated molecules, and an activated complex structure that gives the correct entropy of activation, ΔS^+, as derived from the high-pressure Arrhenius A factor[13] for the appropriate thermal unimolecular reaction.

A sufficient knowledge of E^*, E_0, and activated complex structure is available for CH_3–Si rupture (reactions 5 and 10) and for Si–H rupture (reactions 8 and 12) to carry out meaningful RRKM theory calculations for these processes.[3] It is seen from the footnotes of Table I that the values of k_8, k_{10}, and k_{12} were deduced from rate constant ratios relative to k_5 based on previous theoretical calculations;[3c] thus a direct RRKM theory calculation of the absolute values of k_8, k_{10}, and k_{12} would serve no further purpose.

RRKM Theory Calculation of k_5. The initial calculation of $k_5 \sim k_E^*$ utilizes the older RRKM theory formulation[12a] given by

$$k_E^* = d\left(\frac{I_x^+ I_y^+ I_z^+}{I_x I_y I_z}\right)^{1/2} \frac{\sum_{E^+_{VR}=0}^{E^+} P(E^+_{VR})}{hN(E^*_{VR})} \quad (VI)$$

where d = the reaction path degeneracy, $I_x^+ I_y^+ I_z^+$ = the product of principal moments of inertia for the

(9) R. J. Cvetanovic and L. C. Doyle, *J. Chem. Phys.*, **50**, 4705 (1969).

(10) W. L. Hase, R. L. Johnson, and J. W. Simons, *Int. J. Chem. Kinet.*, **4**, 1 (1972).

(11) I. M. T. Davidson, C. Eaborn, and M. N. Lilly, *J. Chem. Soc. A*, 2624 (1964); I. M. T. Davidson and C. J. L. Metcalfe, *ibid.*, 2630 (1964); I. M. T. Davidson and M. R. Jones, *ibid.*, 5481 (1964); R. N. Hazeldine and J. G. Speight, *Chem. Commun.*, 995 (1967); R. N. Hazeldine, P. J. Robinson, and R. F. Simmons, *J. Chem. Soc. A*, 1890 (1964).

(12) (a) R. A. Marcus and O. K. Rice, *J. Phys. Colloid. Chem.*, **55**, 894 (1951); R. A. Marcus, *J. Chem. Phys.*, **20**, 359, (1952); (b) R. A. Marcus, *ibid.*, **43**, 2658 (1965); E. V. Waage and B. S. Rabinovitch, *Chem. Rev.*, **70**, 377 (1970).

(13) S. Glasstone, K. J. Laidler, and H. Eyring, "Theory of Rate Processes," McGraw-Hill, New York, N. Y., 1941.

activated complex, $I_xI_yI_z$ = the product of principal moments of inertia for the energized molecule, $\sum_{E^+_{VR}=0}^{E^+}$ $P(E^+_{VR})$ = the sum of vibrational-active rotational states for the activated complex up to E^+, $N(E^*_{VR})$ = the density of vibrational-active rotational states for the energized molecule, $E^+ = E^* - E_0$, and E_{VR} = vibrational + active rotational energy. Since previous calculations of Si–CH_3 bond rupture rates utilized this formulation,[3] it is used in our initial calculations for comparative purposes.

The average energy, E^*, of DMS* was determined by the equation

$$E^* = \Delta H_f°_0(\text{MS}) - \Delta H_f°_0(\text{DMS}) + [\Delta H_f°_0(^1CH_2) + E^*(^1CH_2)] + E_{th} \quad \text{(VII)}$$

where $[\Delta H_f°_0(^1CH_2) + E^*(^1CH_2)]$ = 116.1 kcal/mol for CH_2N_2 photolyses at 3660 Å,[14] and E_{th}, the average vibrational and internal rotational thermal energy at 25° of the formed DMS*, was calculated from statistical thermodynamics to be 2.6 kcal/mol. The value of $\Delta H_f°_0(\text{MS}) - \Delta H_f°_0(\text{DMS})$ was determined from

$$\Delta H_f°_0(\text{MS}) - \Delta H_f°_0(\text{DMS}) = D°_{298}(CH_3SiH_2\text{–}CH_3) - D°_{298}(CH_3SiH_2\text{–H}) + \Delta H_f°_{298}(\text{H}) - \Delta H_f°_{298}(CH_3) - 1.5 \text{ kcal/mol} \quad \text{(VIII)}$$

where $\Delta H_f°_{298}(\text{H})$ = 52.0 kcal/mol,[15] $\Delta H_f°_{298}(CH_3)$ = 34.0 kcal/mol,[15] and −1.5 kcal/mol corrects 298°K values to 0°K.[16] A value of −6 ± 4 kcal/mol encompasses the 298°K values of the difference between Si–CH_3 and Si–H bond dissociation energies that can be deduced from the more reliable literature determinations of this and related quantities for various compounds.[17–20] Although some variation of $D(R_3Si\text{–}CH_3) - D(R_3Si\text{–H})$ with the nature of R could exist, the variation is probably small and the available data are insufficiently accurate to demonstrate it. Thus $\Delta H_f°_0(R_3SiH) - \Delta H_f°_0(R_3SiCH_3)$ = 10.5 ± 4 kcal/mol. These quantities combine to give E^* = 129 ± 4 kcal/mol.

The critical energy, E_0, for Si–CH_3 bond rupture was taken to be equivalent to the bond dissociation energy. A value of 78 ± 4 kcal/mol encompasses electron impact bond dissociation energy measurements and thermal activation energy measurements on related compounds.[17,19]

Activated complexes that fitted k_E to k_5 at the E^* and E_0 values above are given in Table II. These complexes were derived by taking an Si–C stretching vibration as the reaction coordinate and lowering four molecular vibrational frequencies, two C–Si–C bending and two CH_3–Si rocking frequencies, by the same factor in the complexes. These factors are 2.06, 3.05, and 4.76 for complexes I, II, and III, respectively. All internal rotors were taken as active and free.

The overall moment of inertia ratio is the same as that used previously and corresponds to extending a

Table II. Theoretical Parameters of DMS Decomposition by C–Si Bond Rupture[a]

Molecule	Complex model I	Complex model II	Complex model III
857	416	281	180
841	409	276	177
469	228	154	99
227	110	75	48
724	r.c.	r.c.	r.c.
$\left(\frac{I_x^+I_y^+I_z^+}{I_xI_yI_z}\right)^{1/2}$	1.60	1.60	1.60
log [A(sec^{-1})/methyl][b]	14.72	15.40	16.17
E_0, kcal/mol	74.0	78.0	82.0
E^*, kcal/mol	133.0	129.0	125.0

[a] Frequencies (cm^{-1}) common to molecule and complexes (I. F. Kovalev, *Opt. Spectrosc.*, **8**, 166 (1960)): 2967 (4), 2899 (2), 2135 (2), 1433 (4), 1267 (2), 949, 915, 882, 868, 760, 655. [b] The log A values are for 1000°K as calculated by absolute rate theory.[13]

Table III. CH_3–Si Bond Rupture Parameters from Revised RRKM Theory

Molecule[a]	Complex models I	Complex models II	Complex models III
	Dimethylsilane		
857	376	247	154
841	372	242	151
469	208	135	85
227	100	66	41
724	r.c.	r.c.	r.c.
log [A(sec^{-1})/methyl]	14.9	15.6	16.4
E_0, kcal/mol	74.0	78.0	82.0
E^*, kcal/mol	133	129	125
k_E, sec^{-1}		0.92×10^9 (3660 Å)	
	Trimethylsilane[3c]		
874	523	313	183
835	501	300	175
244	145	87	51
225	135	81	47
714	r.c.	r.c.	r.c.
log [A(sec^{-1})/methyl]	14.4	15.3	16.2
E_0, kcal/mol	74.0	78.0	82.0
E^*, kcal/mol	134	130	126
k_E, sec^{-1}		2.0×10^7 (3660 Å)	
	Tetramethylsilane[3a]		
869	725	388	199
869	725	388	199
239	200	107	55
202	169	90	47
696	r.c.	r.c.	r.c.
log [A(sec^{-1})/methyl]	13.8	14.9	16.0
E_0, kcal/mol	74.0	78.0	82.0
E^*, kcal/mol	135	131	127
k_E, sec^{-1}		6.5×10^5 (3660 Å)	
E^*, kcal/mol	131.5	127.5	123.5
k_E, sec^{-1}		2.8×10^5 (4358 Å)	
	Ethyltrimethylsilane[3b]		
869	626	312	160
869	626	312	160
239	159	86	44
202	135	73	37
696	r.c.	r.c.	r.c.
log [A(sec^{-1})/methyl]	14.1	15.2	16.4
E_0, kcal/mol	72.0	76.0	80.0
E^*, kcal/mol	123.6	121.6	119.6
k_E, sec^{-1}		1.5×10^4 (4358 Å)	

[a] Frequences unchanged between the molecules and complexes are given in ref 3.

(14) J. W. Simons and G. W. Taylor, *J. Phys. Chem.*, **73**, 1274 (1969); G. W. Taylor and J. W. Simons, *ibid.*, **74**, 464 (1970); G. W. Taylor and J. W. Simons, *Int. J. Chem. Kinet.*, **3**, 25 (1971).
(15) J. A. Kerr, *Chem. Rev.*, **66**, 465 (1966).
(16) American Petroleum Institute Research Project No. 44, Carnegie Institute of Technology, Pittsburgh, Pa., 1944–1952.
(17) S. J. Band, I. M. T. Davidson, and C. A. Lambert, *J. Chem. Soc. A*, 2068 (1968), and references therein; M. F. Lappert, J. Simpson, and T. R. Spalding, *J. Organometal. Chem.*, **17**, 1 (1969).
(18) P. Potzinger and F. W. Lampe, *J. Phys. Chem.*, **74**, 719 (1970).
(19) I. M. T. Davidson and C. A. Lambert, *J. Chem. Soc. A*, 882 (1971); D. F. Helm and E. Mack, Jr., *J. Amer. Chem. Soc.*, **59**, 60 (1937).
(20) M. Y. Agarunov and S. N. Hadzhiev, *Dokl. Akad. Nauk SSSR*, **185**, 577 (1969); S. Tannenbaum, *J. Amer. Chem. Soc.*, **76**, 1027 (1954).

CH_3–Si bond in the activated complex a factor of 1.3. The reaction path degeneracy for C–Si bond rupture in DMS is 2. The evaluation of the sums and densities in eq VI was for harmonic oscillators utilizing the accurate approximation of Whitten and Rabinovitch.[21]

The CH_3–Si rupture parameters for DMS in Table II can be summarized as log [A(sec^{-1})/methyl] = 15.4 ± 0.7 and E_0 = 78 ± 4. This compares favorably with 15.1 ± 0.7 and 78 ± 4 for CH_3–Si rupture in $(CH_3)_3SiH$,[3c] 14.7 and 78 ± 4 for CH_3–Si rupture in $(CH_3)_4Si$,[3a] and 15.2 ± 0.7 and 76 ± 4 for CH_3–Si rupture in $C_2H_5Si(CH_3)_3$.[3b] The rather large uncertainties in these log A values reflect our estimates of the uncertainties in E_0, E^*, and experimental k_E values. The E^* values used for the $(CH_3)_3SiH^*$ and $(CH_3)_4Si^*$ calculations were also based on the value of $D°_{298}(R_3Si-CH_3) - D°_{298}(R_3Si-H) = -6 \pm 4$ kcal/mol. The E^* value for $C_2H_5Si(CH_3)_3^*$ is considerably less uncertain since $\Delta H_f°_0(XCH_3) - \Delta H_f°_0(XCH_3CH_3) = 3.5 \pm 0.5$ kcal/mol for a variety of X groups.

We conclude from the above that the experimental value of k_5 deduced here (Table I) is consistent with other chemical activation data for CH_3–Si bond rupture.

Results for New RRKM Theory Formulation. RRKM theory has been revised so as to treat the adiabatic rotations more accurately.[12b] The revised expression for k_E (see eq VI) drops the ratio $(I_x^+I_y^+I_z^+/I_xI_yI_z)^{1/2}$ from eq VI and E^+ becomes $E^+ = E^* - E_0 + \langle E_J^* \rangle - \langle E_J^+ \rangle$, where $\langle E_J^* \rangle - \langle E_J^+ \rangle$, the difference between the average thermal energies in the adiabatic rotations of the molecule and activated complex, is approximated by

$$\langle E_J^* \rangle - \langle E_J^+ \rangle = \left[\left(\frac{I_x^+I_y^+I_z^+}{I_xI_yI_z}\right)^{1/2} - 1\right]RT$$

corresponding to $l = 2$ and $I_z^+/I_z \sim 1$, which yields 0.36 kcal/mol for the case in question.

This revised treatment leads to slightly "looser" activated complexes for all of our CH_3–Si bond rupture calculations.[22] Activated complexes that fit the revised theory to existing experimental k_E values for CH_3–Si bond rupture reactions in various alkylsilanes are presented in Table III. The main conclusions are unaltered by these revised calculations. Models I and III represent "tightest" and "loosest" complexes, respectively, based on liberal uncertainty estimates in E_0, E^*, and k_E values.

Appendix

The collision frequences of A* (DMS* and ES*) with various bath molecules, B, were calculated by the standard gas kinetic theory relationship

$$W_{A^*B} = \left(\frac{S_{A^*} + S_B}{2}\right)^2\left(\frac{M_{A^*} + M_B}{M_{A^*}M_B}\right)^{1/2}(8\pi kT)^{1/2}N_B$$

which becomes at 300°K

$$W_{A^*B} = 0.255 \times 10^8\left(\frac{S_{A^*} + S_B}{2}\right)^2\left(\frac{M_{A^*} + M_B}{M_{A^*}M_B}\right)^{1/2}P(\text{cm})$$

where S is the effective molecular collision diameter[23] in Å and M is the molecular weight. Values of S for each molecule in this study were determined from Lennard-Jones hard sphere diameters, σ, utilizing the equation, $S = \sigma[\Omega^{2,2*}(kT/\epsilon)]^{1/2}$.[23] σ values for alkylsilanes were estimated by assuming that a Si atom contributes to the equivalent of two C atoms to the σ value of the corresponding alkane. S values are given in Table IV for the molecules of interest in this work.

Table IV. Collision Diameters

Molecule	S, Å	Molecule	S, Å
Dimethylsilane	6.6	Butadiene	6.6
Ethylsilane	6.6	*n*-Butane	6.6
Methylsilane	6.1	Oxygen[a]	3.6
Diazomethane	5.5		

[a] A collisional deactivation efficiency factor of 0.25 for oxygen was included in calculating its collision frequency.

(21) G. Z. Whitten and B. S. Rabinovitch, *J. Chem. Phys.*, **38**, 2466 (1963); **41**, 1883 (1964); D. C. Tardy and B. S. Rabinovitch, *ibid.*, **48**, 1427 (1968).

(22) In our previous work[3] we incorrectly deduced that the results were virtually identical between the original and revised treatments of adiabatic rotations for CH_3–Si rupture calculations.

(23) S. C. Chan, B. S. Rabinovitch, J. T. Bryant, L. D. Spicer, T. Fujimoto, Y. N. Lin, and S. P. Pavlon, *J. Phys. Chem.*, **74**, 3169 (1970), and references therein.